Vol.5 No.1 Jan 2022

Journal of Computational Mechanics, Power System and Control

Received 31 August, Revised 19 October, Accepted 22 November

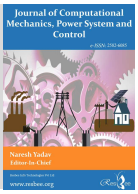

Navigation Control using Fractional Rider Optimization Algorithm for Autonomous Sailing Robots

G.Gokulkumari
Department of E-Commerce, Saudi Electronic University, Kingdom of Saudi Arabia

Abstract: Generally, an autonomous sailing robot is a novel kind of green ship which exploits wind energy in order to preserve the incessant cruising operations. Here, the path planning issue of autonomous sailing robots is performed by exploiting the adopted "Fractional Rider Optimization Algorithm (FROA)". The term FROA is the modification of ROA with fractional theory, and the final aim of the adopted model is to set an optimal path for the autonomous sailing robot. Here, an enhanced mathematical technique was exploited to track the navigation control of a sailing ship. By exploiting a downsized prototype, the navigation is examined for an autonomous sailing robot. Here, the proposed method can increase the entire iterative convergence speed as well as minimize the probability that population will reduce to a locally optimal solution. Finally, experimentation outcomes show the effectuality, robustness, and possibility of the proposed FROA model in diverse scenarios. Moreover, this study presents few references and also provides concepts for navigation control model of autonomous sailing robots

Keywords: Autonomous, Optimization Algorithm, Optimal Path, Robots, Sailing, Ship.

1. Introduction

Nowadays, an increasing activity regarding autonomous surface vehicles is prominent. Such vehicle applications such as reconnaissance, mines countermeasure, port protection, and surveillance mission [1]. Almost certainly a significant reason, which can describe this rising activity, is the actual requirement for enhanced understanding of the complicated communications among the oceans as well as atmosphere and monitoring of the environment [2]. Meteorological, global warming and ecological researchers in specific requirement enhanced characterization of ocean processes and subsequently need an extensive observational tools spectrum to comprehend complicated dynamic coupling among Earth's atmosphere and oceans [5].

In current years, autonomous sailboat robots have received huge notice from numerous researchers as confirmed by the several projects commenced wide-reaching. From the wind, the propulsion is directly extracted for these kinds of vehicles, with only a minute number of energy required to trim sails [6]. Additionally, they can be operated with energy harvesting systems like wind turbines or solar panels. Because of this minimum energy utilization for instances of "power budget, these robots are the striking solution for long-term autonomy and they can be utilized for semi-persistent" attendance as well as monitoring or observation missions in the oceans [3]. Nevertheless, autonomous sailboat control is challenging as the thrust force is based upon the accuracy of uncontrollable as well as partially unpredictable wind. In addition, such vehicles show complicated behavior because of the hydro-aero dynamic properties of their hull and sails. Nevertheless, as the propulsion sailboat source is generally complicated as well as the sailboat is subjected to other arbitrary forces like waves and currents, its dynamics are extremely non-linear creating its automatic control a non-trivial issue. Specifically, the path planning techniques are concentrated used for common mobile robots are not work similarly in this type of autonomous vehicle. For instance, the technique adopted based on reinforcement learning such as the Q-learning approach that is adopted and exploited on smart motorized ships does not use in straight experimentation. It is very complicated to exploit a technique for sailboats, which are motorized boats that do not require considering the wind direction [7]. Auspiciously, by exploiting a sort of punishment, this constraint can be integrated into the Q-Learning technique. Therefore, the Markovian decision procedure is enabled by exploiting a similar technique to develop a path planning for a sailboat [3].

In general, the conventional path planning techniques can be categorized into 2 classifications such as

https://doi.org/10.46253/jcmps.v5i1.a5

traditional approaches, Metaheuristic optimization approaches [13]. Traditional approaches such as artificial potential fields, cell decomposition, as well as sampling-based approaches. Nevertheless, traditional techniques are time utilizing and need adequate storage memory. Meta-heuristic approaches have turned out to be well-liked because of their flexibility and stability as well as their capability to enhance and keep away from local optimizations. Therefore, Metaheuristic optimization techniques are exploited often to optimize path planning issues. Aforesaid approaches can be categorized into evolution-based, physics-based, swarm-based, and human-based approaches [13] and [14].
The main objective of this paper is stated as below:

- Initially, on the basis of the enhanced mathematical formulation of the sailing the sailboat navigation control is ascertained.
- Subsequently, the FROA optimization model is exploited for path planning issue of autonomous sailing robots.
- Finally, experimentation is conducted for both the proposed and conventional models.

The organization of the paper is as follows: Section 2 demonstrates the description of an autonomous sailing robot system. Section 3 explains the proposed model for Path planning. Section 4 demonstrates the result and analysis. Section 5 concludes the paper.

2. Description of an Autonomous Sailing Robot System

2.1 Sailboat Kinematics and Dynamics

In this section, the dynamics of a 4degree-of-freedom sailboat are described. Eq. (1) states the surge formulation, eq. (2) states the formulation of sway, eq. (3) states the formulation of roll and eq. (4) states the formulation of Yaw, where X and Y represents the force components along an axis, v indicates the mass, L and M indicates velocity components of the boat, and ψ represents heading angle [7].

$$(v+v_x)\dot{L}-\left(v+v_y\cos^2\psi+v_z\sin^2\psi\right)M\dot{\psi}=X_0+X_H+X_{V_\psi}.M\dot{\psi}+X_R+X_S \tag{1}$$

$$\left(v+v_y\cos^2\psi+v_z\sin^2\psi\right)\dot{M}+(v+v_x)\dot{L}\psi+2(v_Z-v_y)\sin\psi\cos\psi\bullet M\psi=Y_H+Y_{\dot{\psi}}\dot{\psi}+Y_{\dot{\psi}}\dot{\psi}+Y_R+Y_S \tag{2}$$

$$\left(v+v_y\cos^2\psi+v_z\sin^2\psi\right)\dot{M}+(v+v_x)\dot{L}\psi+2(v_z-v_y)\sin\psi\cos\psi\bullet M\psi=Y_H+Y_{\dot{\psi}}\dot{\psi}+Y_{\dot{\psi}}\dot{\psi}+Y_R+Y_S \tag{3}$$

$$\left\{(I_{yy}+J_{yy})\sin^2\psi+(I_{zz}+J_{zz})\ddot{\psi}\cos^2\psi\right\}+2\left\{(I_{yy}+J_{yy})-(I_{zz}+J_{zz})\ddot{\psi}\cos^2\psi\right\}\sin\psi\cos\psi\bullet\dot{\psi}\dot{\psi}=N_H+N_{\dot{\psi}}\dot{\psi}+N_R+N_S \tag{4}$$

The steady forces on the fin keel and canoe body are explained by exploiting below hydrodynamic derivatives:

$$Y_H=\left(Y'_M M'+Y'_\psi\psi+Y'_{M\psi\psi}M'^2\psi+Y'_{MM}M'^3\right)\left(\frac{1}{2}\rho M_B^2 ld\right) \tag{5}$$

$$X_H=\left(X'_{MM}M'_2+X'_{\psi\psi}\psi^2+X'_{MMM}M'^2\right)\left(\frac{1}{2}\rho M_B^2 ld\right) \tag{6}$$

$$K_H=\left(K'_M M'+K'_\psi\psi+K'_{M\infty}M'^2\psi+K'_{MM\psi}M'^2\psi+K'_{MM}M'^3\right)\times\left(\frac{1}{2}\rho M_B^2 ld^2\right) \tag{7}$$

$$K_H=\left(K'_M M'+K'_\psi\psi+K'_{M\infty}M'^2\psi+K'_{MM\psi}M'^2\psi+N'_{MM}M'^3\right)\times\left(\frac{1}{2}\rho M_B^2 ld^2\right) \tag{8}$$

Where, ρ indicates water density, δ indicates rudder angle.

$$M'=-\frac{M_B\sin\beta}{M_B}=-\sin\beta \tag{9}$$

The moments on rudder and hydrodynamic forces are indicated as

$$X_R=C_{X\delta}\sin\alpha_R\sin\delta\left(\frac{1}{2}\rho M_B^2 ld^2\right) \tag{10}$$

$$Y_R = C_{Y\delta} \sin\alpha_R \cos\delta \cos\delta \left(\frac{1}{2} \rho M_B^2 l d^2 \right) \tag{11}$$

$$K_R = C_{K\delta} \sin\alpha_R \cos\delta \left(\frac{1}{2} \rho M_B^2 l d^2 \right) \tag{12}$$

$$N_R = C_{N\delta} \sin\alpha_R \cos\delta \cos\psi \left(\frac{1}{2} \rho M_B^2 l d^2 \right) \tag{13}$$

$C_{X\delta}$ to $C_{N\delta}$ indicate coefficients ascertained from rudder angle tests. The α_R indicates effectual attack angle of the rudder, which is stated as follows:

$$\alpha_R = \delta - \gamma R \cdot \beta - \tan^{-1}\left(\frac{1 R \dot{\psi}}{L} \right) \tag{14}$$

γR indicates the minimizing inflow angle ratio that is mostly occurred by downwash from fin keel.

As mentioned before, it mostly develops mathematical formulation of a sailboat; enhances parameters to improve suit.

2.2 Track Navigation Control

In this paper, the mathematical formulation of the sailboat is explained to understand the tracking of navigation control. Generally, tracking of navigation control includes the sailing rudder as well as sailboat rudder tracking. Here, 2 separate "Single Input Single Output (SISO)" are presumed to control the sail and rudder, which are independent of each other. A low order controller development to direct a sailboat to its acquired position is a comparatively simple task, generally resolved using an easy, static "proportional integral differential (PID) course controller". In general, the process can be simply set by PID controller. Usually, it is acquired for a sailboat to exploitstatic set control parameters that aretypically establish during "trial and error", all through the missionto attain target position.

2.3. Small Autonomous Sailing Robot

The benefit of a "small-scale sailboat is it can have large ship behavior", which is simple to examine [4]. The ATK-S1216F8-BD is adopted by the sailing robot GPS, which possesses maximum performance that is based upon the ALIENTEK, which is exploited to position the current location of the sailboat and present data for the computation of the control and data. The minimum-cost module GY953 is exploited by the electronic compass. An accelerator sensor and gyroscope are exploited in this compass; via the data fusion approach, the magnetic field sensor attains direct angle data, which directly outcome the heading angle. A high-precision single revolves around a wind vane and an absolute encoder consists of the wind direction sensor. Using raspberry, all electronic devices are controlled. Here, 2 modes of operation are performed by the autonomous sailing boat such as manual and automatic modes the sailboat can sail autonomously, and the remote control is used for the operation.

Fig 1 demonstrates the model of autonomous sailing robot software that can be partitioned into 4 important types. In order to collect the environmental data and internal state, the perceptual modules are exploited. Here, the environmental data comprise the information on wind direction. Then, the internal data comprises information on the rudder and sail angle, as well as the sailboat's absolute location. The control module controls the rudder and sails angle.

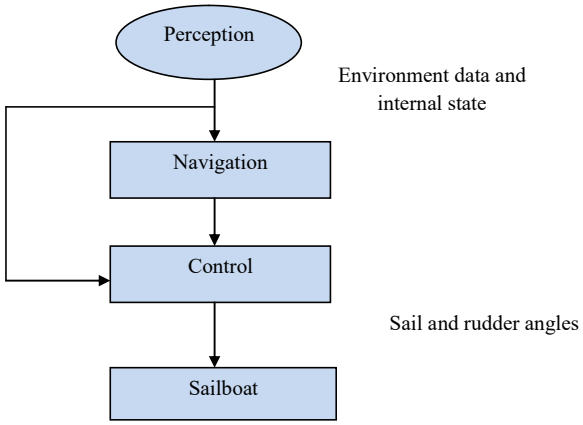

Fig. 1. Systematic model of autonomous sailing robot

3. Proposed Model for Path planning

The path planning approach is on the basis of the FROA approach. Initializes the four-rider groups as J. Initialize the rider position randomly. $K_{x,y}^{\tau}$ represents y^{th} location solution of x^{th} rider at an instant τ. Here, followers F, a total of R riders so that R and J are equivalent, bypass riders B, G indicates riders' location, and the total riders are the summation of the riders in the individual rider groups, over takers O, and attackers A [10].

$$K_{\tau} = \left\{K_{x,y}^{\tau}\right\}; 1 \le x \le R; 1 \le y \le G \tag{15}$$

Therefore, the total riders are stated in eq. (16), Eq. (17) states the condition indicates relation amid the riders to calculate their location [11].

$$R = B + F + O + A \tag{16}$$

$$B = F = O = A = R/4 \tag{17}$$

The location range of follower, overtaker, bypass, and attacker riders lies in the range of $\left[K_1, K_{R/4}\right]$, $\left[K_{R/4+1}, K_{R/2}\right]$, $\left[K_{R/2+1}, K_{3R/4}\right]$, and $\left[K_{3R/4}, K_R\right]$, correspondingly.

Rider parameters, accelerator, steering, gear, as well as brake change on basis of vehicle they employ either car or automobile, and these parameters. Eq. (18) states that the steering angle $(\varphi)$of rider at a time τ, $\varphi_{\tau}(x,y)$indicates the vehicle steering angle of x^{th} rider, at first it is stated that the steering angle is "0".

$$\varphi_{\tau} = \left\{\varphi_{\tau}(x,y)\right\}; 1 \le x \le R; 1 \le y \le G \tag{18}$$

Eq. (19) states the steering angle at a time τ, φ_x^{pos} indicating the vehicle position angle for x^{th} rider. Eq. (20) indicates the computation of the utmost location angle, which is 360^0 the position angle, φ_y^{cor} indicates y^{th} rider coordinate angle, and the most important role is to compute the steering angle. Eq. (21) indicates the coordinate angle is given in quadrants.

$$\varphi_{\tau}(x,y) = \varphi_x^{pos} + \varphi_y^{cor} \tag{19}$$

$$\varphi_x^{pos} = x * \frac{360^{\circ}}{R} \tag{20}$$

$$\varphi_y^{cor} = \begin{cases} 90^{\circ} & ;\text{if} \varphi_x^{pos} \le 90^{\circ} \\ 180^{\circ} & ;\text{if } 90^{\circ} \le \varphi_x^{pos} \le 180^{\circ} \\ 270^{\circ} & ;\text{if } 180^{\circ} \le \varphi_x^{pos} \le 270^{\circ} \\ 1 & ;\text{if } 270^{\circ} \le \varphi_x^{pos} \le 360^{\circ} \end{cases} \tag{21}$$

In the case of location angle, the coordinate angle 90^0 relies below on or equivalent to 90^0. Eq. (22) indicates the rider gear in a group, γ_x indicates x^{th} rider gear. At first, γ_x is set to "0", gear of x^{th} rider γ_x

obtains a value amid "0 and 4". In eq. (23), x^{th} rider's vehicle accelerator is mentioned, ω_x indicating x^{th} rider accelerator which relies on among "0 and 1". The x^{th} rider's vehicle brake is represented in eq. (24), β_x indicates x^{th} riders' vehicle brake and $(0 \le \beta_x \le 1)$. At first, the brake β_x value is "1". The speed set up by a rider to target, as well as regulation in speed is based upon boundaries in space that is minimum coordinates K_{min} and maximum coordinates K_{max}. Hence, the utmost speed of the rider is mentioned in eq. (25), τ_{off} indicates off-time or utmost time and S_{max} is the utmost speed of the riders' vehicle. The vehicle gear speed limit is stated eq. (26), $|\gamma|$ indicates total gears.

$$\gamma = \{\gamma_X\}; 1 \le x \le R \tag{22}$$

$$\omega = \{\omega_X\}; 1 \le x \le R \tag{23}$$

$$\beta = \{\beta_X\}; 1 \le x \le R \tag{24}$$

$$S_{max} = \frac{K_{max} - K_{min}}{\tau_{off}} \tag{25}$$

$$S^{\gamma} = \frac{S_{max}}{|\gamma|} \tag{26}$$

By the success rate, the winner is ascertained. The rider with the utmost success rate is leading rider, as well as maximum success rate, stands for minimum distance on the basis of destination. Conversely, a leader is not constantly as similar as changes regarding time.

The riders' location ahead bypassing the rider concerning the leader's location, is updated arbitrarily as eq. (27), η indicates an arbitrary number in $[0,1]$ with size $[1,R]$, υ and ν indicates arbitrary numbers in [0, 1] and $[1, R]$. Likewise, ϖ represents a constant for selecting a value in $[1,R]$. Therefore, the location for winning the race is updated by the individual rider. The alteration of the developed formulation is inherited by exploiting the fraction idea that involves the optimal solution of the preceding iterations for a location update.

$$K^{B}_{\tau+1}(x,y) = \upsilon\left[K_{\tau+1}(\nu,y) * \eta(y) + K_{\tau}(\varpi,y) * [1 - \eta(y)]\right] \tag{27}$$

Rearranging the eq. (28) as,

$$K^{B}_{\tau+1}(x,y) = \upsilon * K_{\tau}(\nu,y) * \eta(y) + \upsilon * K_{\tau}(\varpi,y) - \upsilon * \eta(y) * K_{\tau}(\varpi,y) \tag{28}$$

Consider that $\nu = \varpi = x$ so that the aforesaid formulations turn out to be, as eq. (29).

$$K_{\tau+1}(x,y) = \upsilon * K_{\tau}(x,y) \tag{29}$$

By exploiting $K_{\tau}(x,y)$ subtracting on both sides to implement the fractional idea,

$$K_{\tau+1}(x,y) - K_{\tau}(x,y) = \upsilon * K_{\tau}(x,y) - K_{\tau}(x,y) \tag{30}$$

$$K_{\tau+1}(x,y) - K_{\tau}(x,y) = (\upsilon - 1) * K_{\tau}(x,y) \tag{31}$$

$$\partial^{\alpha}\left[K_{\tau+1}(x,y)\right] = (\upsilon - 1) * K_{\tau}(x,y) \tag{32}$$

$\partial^{\alpha}\left[K_{\tau+1}(x,y)\right]$ represents fractional term which can be reformulated as

$$K_{\tau+1}(x,y) - \alpha . K_{\tau}(x,y) - \frac{1}{2} \times \alpha \times K_{\tau-1}(x,y) - \frac{1}{6} \times (1-\alpha) \times K_{\tau-2}(x,y) - \frac{1}{24} \times \alpha \times (1-\alpha)(2-\alpha) K_{\tau-3}(x,y) = (\upsilon - 1) * K_{\tau}(x,y) \tag{33}$$

$$K_{\tau+1}(x,y) = (\alpha + \delta - 1). K_{\tau}(x,y) + \frac{1}{2} \times \alpha \times K_{\tau-1}(x,y) + \frac{1}{6} \times (1-\alpha) \times K_{\tau-2}(x,y) + \frac{1}{24} \times \alpha \times (1-\alpha)(2-\alpha) K_{\tau-3}(x,y) \tag{34}$$

$K_{\tau-1}(x,y)$, $K_{\tau-2}(x,y)$, and $K_{\tau-3}(x,y)$ represents the optimal location of the x^{th} rider in preceding iterations, as well as these solutions, are incidental to updating rider location in attendance iteration.The location is updated by the follower based on the leading rider to arrive at target rapidly which is on the basis of the selected coordinates. The location update is mentioned in eq. (35), ∂^{τ}_{x} indicates distance to be covered by x^{th} rider that is the product of rider velocity V^{τ}_{x} and g represents co-ordinate selector, $\varphi^{g}_{t}(x,y)$ represents x^{th} rider steering angle in g^{th} co-ordinate, $K^{L}(g)$ represents leading rider location, and τ_{off} indicates off-time rate as given as eq. (36).

$$K^{F}_{\tau+1}(x,g) = K^{L}(g) + \left[\cos\left(\varphi^{g}_{t}(x,y)\right) * K^{L}(g) * \partial^{\tau}_{x}\right] \tag{35}$$

$$\partial_{x}^{\tau} = V_{x}^{\tau} * \left(\frac{1}{\tau_{off}} \right) \tag{36}$$

The velocity of rider is based upon rider parameters and vehicle speed and not on steering angle eq. (37), S_{max} indicates the utmost rider's speed vehicle. The parameters, like accelerator, gear, the brake of a vehicle of x^{th} rider, γ_{x}^{τ}, ω_{x}^{τ} and β_{a}^{τ} correspondingly. On the basis of the on-time probability, the coordinate selector depends as stated in (38).

$$V_{x}^{\tau} = \frac{1}{3x}\left[\gamma_{x}^{\tau} * S^{\gamma} + S_{max} * \omega_{x}^{\tau} + \left(1-\beta_{a}^{\tau}\right) * \omega_{x}^{\tau}\right] \tag{37}$$

$$\rho_{ON}^{\tau} = \left(\frac{\tau}{\tau_{off}} \right) * G \tag{38}$$

The coordinate selector selects a value based on meeting the below circumstance in eq. (39), ρ_{on}^{τ} indicates on-time probability.

$$g << \left\{ \left(y * \rho_{on}^{\tau} \right); \quad \text{if} \left(y * \rho_{on}^{\tau} \right) < G \ \ \forall y \right. \tag{39}$$

Based on coordinate selector, overtaker position is updated, relative success rate, and direction indicator, $D_{\tau}(x)$ indicates indicator showing the i^{th} rider direction at τ, and $K_{\tau}(x,y)$ indicates x^{th} rider location, it is calculated by exploiting rider relative success rate is stated in eq. (41).

$$K_{\tau+1}^{O}(y,g) = K_{\tau}(x,y) + \left[D_{\tau}(x) * K^{L}(g) \right] \tag{40}$$

$$D_{\tau}(x) = \left[\frac{2}{1 - \log\left(\eta_{r}^{\tau}(x) \right)} \right] - 1 \tag{41}$$

$\eta_{r}^{\tau}(x)$ indicates x^{th} rider relative success rate at τ which represents success rates ratio of x^{th} rider, $\eta_{r}^{\tau}(x)$ to utmost success rate attained with any of R riders. To decide a value in direction indicator $D_{\tau}(x)$, relative success rate deviates in $[0,1]$ that deviates in $[1,-1]$. $\partial_{norm}(x,y)$ represents coordinate selector, which is based upon "normalized distance-vector" that indicates the distance among t x^{th} rider locations and leading rider as stated as eq. (43), $K_{\tau}(x,y)$ and $K^{L}(y)$ indicates x^{th} rider as well as leading rider locations. Hence, coordinate selector determines a value from y to assure the below circumstance as stated in eq. (44).

$$\eta_{r}^{\tau}(x) = \frac{\eta_{r}(x)}{\max\limits_{x=1}^{R} r(x)} \tag{42}$$

$$\partial_{norm}(x,y) = \left| K_{\tau}(x,y) - K^{L}(y) \right| \tag{43}$$

$$g << \left\{ y \ ; \text{ if } \partial_{norm}(x,y) < m\left(\partial_{norm}(x)\right) \right. \quad \forall y \tag{44}$$

To reach your destination at the leader's location, the attacker is like the follower endeavoring. The attacker location is stated as eq. (45), $K^{L}(y)$ indicates leading rider location, and in y^{th} coordinate the steering angle of x^{th} rider, $\varphi_{\tau}(x,y)$, and ∂_{x}^{y} indicates the distance to be performed using the x^{th} rider.

$$K_{\tau+1}^{A}(x,y) = K^{L}(y) + \left[\cos\left(\varphi_{\tau}(x,y) \right) * K^{L}(y) \right] + \partial_{x}^{y} \tag{45}$$

The success rates are updated once the location update concludes, to confirm the winner, obtaining the utmost success rate. On the basis of the activity counter, best solution is based upon the rider parameters like gear and steering angle are updated that is based on the successive rate. The activity counter $C^{\tau+1}(x)$ turns out to be one while the success rate of x^{th} rider at τ is higher than success rate of x^{th} rider at $(\tau+1)$.

$$C^{\tau+1}(x) = \begin{cases} 1 \ ; \text{ if } r_{\tau}(x) > r_{\tau-1}(x) \\ 0; \text{ otherwise} \end{cases} \tag{46}$$

On the basis of $C^{\tau+1}(x)$, the steering angle is updated as eq. (47).

$$\varphi_{\tau+1}(x,y) = \begin{cases} \varphi_{\tau}(x+1,y) \ ; \text{ if } C^{\tau+1}(x) = 1 \\ \varphi_{\tau}(x-1,y); \text{ if } C^{\tau-1}(x) = 0 \end{cases} \tag{47}$$

Based upon the activity counter, eq. (48) states the gear for the instant $(\tau+1)$ is updated.

$$\gamma_x^{\tau+1} = \begin{cases} \gamma_x^{\tau+1} + 1 \; ; \text{ if } C^{\tau+1}(x) = 1 \\ \gamma_x^{\tau+1} - 1; \text{ if } C^{\tau+1}(x) = 0 \\ \gamma_x^{\tau} \quad ; \text{ if } \gamma_x^{\tau} = |\gamma| \end{cases} \tag{48}$$

Based on the gear, accelerator is updated using eq. (49), $|\gamma|$ is the number of gears.

$$\omega_x^{\tau} = \frac{\gamma_x^{\tau+1}}{|\gamma|} \tag{49}$$

Eq. (50) states the update in brake is like that of an accelerator.

$$\beta_x^{\tau+1} = \left[1 - \frac{\gamma_x^{\tau+1}}{|\gamma|}\right] \tag{50}$$

4. Result and Analysis

In this section, experimentation of adopted and conventional models like "Particle Swarm Optimization (PSO), Artificial Bee Colony (ABC), and Beetle Swarm Optimization (BSO)" was demonstrated. Here, the main aim of the experimentation was to examine the control modules and navigation for the sailboat without the obstruction recognition module. In the experimentation, four cases were exploited it was performed on the basis of the initial points, destination points, and obstacle points.

Fig 2 demonstrates a statistical analysis of adopted as well as existing techniques for four cases. Here, the experimentation outcomes demonstrate that the proposed model attains the least value with respect to the best, median, mean, and standard deviation. Therefore, the overall analysis states the superiority of adopted as well as existing techniques.

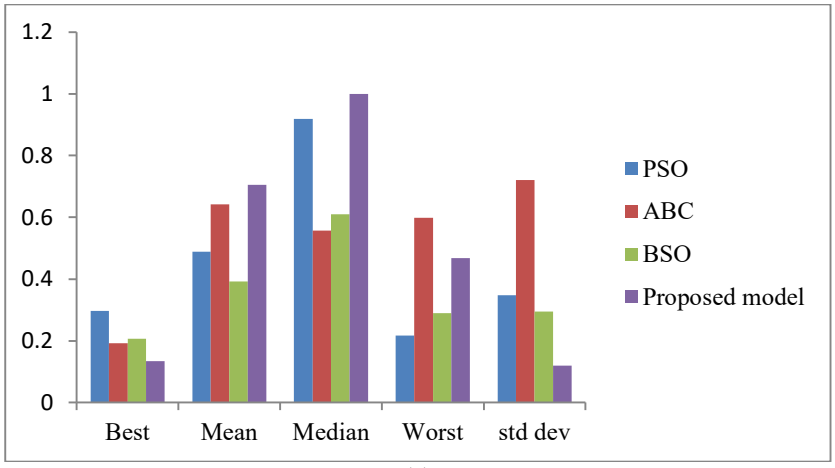

(a)

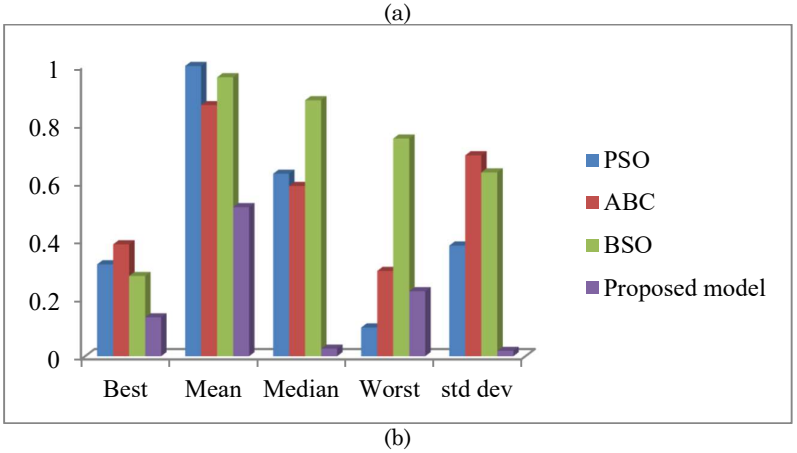

(b)

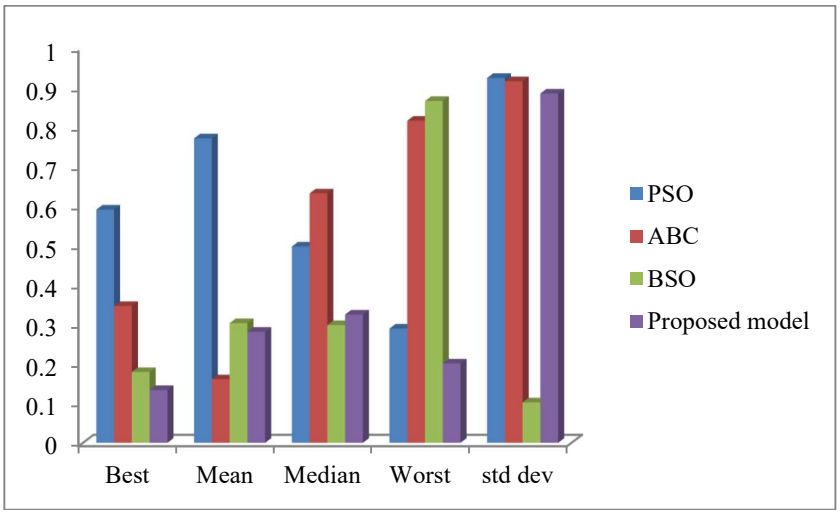

(c)

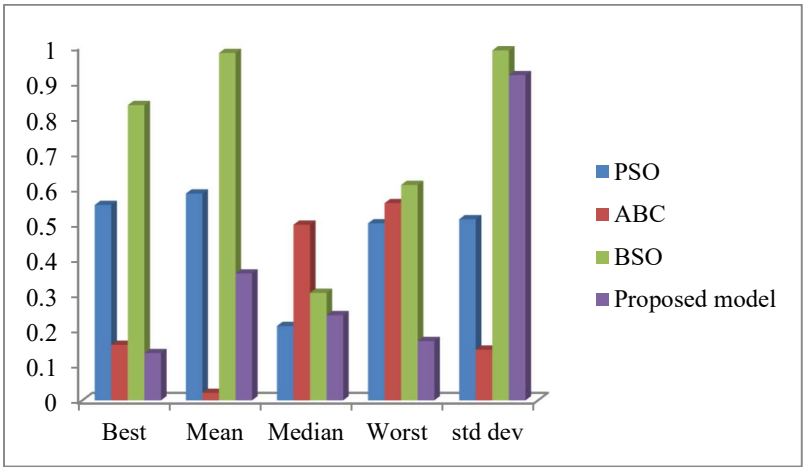

(d)

Fig. 2. *Statistical analysis of the proposed and conventional models (a) case 1; (b) case 2; (c) case 3; and (d) case 4*

Table 1 demonstrates the time complexity of the proposed and conventional models that measure the time for the function to run the approaches. Here, 2 parameters are set such as D represents the parameter dimension; N represents the population size.

Table 1: *Comparative analysis of proposed and conventional models regarding computational complexity*

Methods	Computational Complexity
PSO	O(ND)
ABC	O(ND)
BSO	O(ND)
Proposed	O(ND)

5. Conclusion

In this paper, the experimentation on the basis of the mathematical formulation of an autonomous navigation robot was performed. To drive the autonomous navigation robot the controller was effectually exploited by using the modeled route. In a sea area, navigation was examined on the sailboat was performed. Here, the FROA optimization model was exploited for the path planning issue of autonomous sailing robots. Moreover, inertia weight formulation, as well as step size factor, was dynamically changed. For autonomous sailing robots, the proposed model permits obstruction evasion path planning. Here, the main 2 features were evaluated: the initial feature was the performance of the path planning that was calculated by the planning approach, and the next one was calculated using the computational complexity for the computational performance.

Compliance with Ethical Standards

Conflicts of interest: Authors declared that they have no conflict of interest.

Human participants: The conducted research follows the ethical standards and the authors ensured that they have not conducted any studies with human participants or animals.

References

[1] Clement Petres, Sorbonne Universite, Miguel-Angel and Romero-Ramirez, "Modeling and reactive navigation of an autonomous sailboat", Conference: 2011 IEEE/RSJ International Conference on Intelligent Robots and Systems, IROS 2011, San Francisco, CA, USA, September 25-30, 2011.

[2] Hadi Saoud, Minh-Duc Hua, Frederic Plumet, Faïz BEN Amar, "Modeling and reactive navigation of an autonomous sailboat", Conference: 2011 IEEE/RSJ International Conference on Intelligent Robots and Systems, IROS 2011, San Francisco, CA, USA, September 25-30, 2011.

[3] K. Isaka, K. Tsumura, T. Watanabe, W. Toyama, M. Sugesawa, Y. Yamada, H. Yoshida, and T. Nakamura, "Development of underwater drilling robot based on earthworm locomotion," IEEE Access, vol. 7, pp. 103127–103141, 2019.

[4] R. A. S. Fernandez, D. Grande, A. Martins, L. Bascetta, S. Dominguez, and C. Rossi, "Modeling and control of underwater mine explorer robot UX-1," IEEE Access, vol. 7, pp. 39432–39447, 2019.

[5] K. Isaka, K. Tsumura, T. Watanabe, W. Toyama, M. Sugesawa, Y. Yamada, H. Yoshida, and T. Nakamura, "Development of underwater drilling robot based on earthworm locomotion," IEEE Access, vol. 7,pp. 103127–103141, 2019.

[6] D. Ribas, P. Ridao, A. Turetta, C. Melchiorri, G. Palli, J. J. Fernandez, and P. J. Sanz, "I-AUV mechatronics integration for the TRIDENT FP7 project," IEEE/ASME Trans. Mechatronics, vol. 20, no. 5, pp. 2583–2592, Oct. 2015.

[7] L. Zhou, K. Chen, H. Dong, S. Chi and Z. Chen, "An Improved Beetle Swarm Optimization Algorithm for the Intelligent Navigation Control of Autonomous Sailing Robots," in IEEE Access, vol. 9, pp. 5296-5311, 2021.

[8] H. Erckens, G.-A. Busser, C. Pradalier, and R. Y. Siegwart, "Avalon: Navigation strategy and trajectory following controller for an autonomous sailing vessel," IEEE Robot. Autom. Mag., vol. 17, no. 1, pp. 45–54, Mar. 2010.

[9] M. Romero, Y. Guo, S.-H. Ieng, F. Plumet, R. Benosman, and B. Gas, "Omni-directional camera and fuzzy logic path planner for autonomous sailboat navigation," in Proc. Iberoamer. Conf. Electron. Eng. Comput. Sci., 2011, pp. 335–346.

[10] D.Binu and B. S.Kariyappa, "RideNN : A New Rider Optimization Algorithm-Based Neural Network for Fault Diagnosis in Analog Circuits," IEEE Trans. Instrum.Meas., pp. 1–25, 2018.

[11] Arikrishnaperumal Ramaswamy Aravind,Rekha Chakravarthi,"Fractional rider optimization algorithm for the optimal placement of the mobile sinks in wireless sensor networks",vol.34, no. 4, 10 March .

[12] Mr. Rupam Gupta Roy,"Economic Dispatch Problem in Power System Using Hybrid PSO and Enhanced Bat Optimization Algorithm", Journal of Computational Mechanics, Power System and Control, vol.3, no.3, July 2020

[13] Rajeshkumar G,"Hybrid Particle Swarm Optimization and Firefly Algorithm for Distributed Generators Placements in Radial Distribution System", Journal of Computational Mechanics, vol.2, no. 1, January 2019